

## ORIGINAL ARTICLE

## RAF kinase inhibitor-independent constitutive activation of Yes-associated protein 1 promotes tumor progression in thyroid cancer

SE Lee<sup>1,7</sup>, JU Lee<sup>2,7</sup>, MH Lee<sup>1</sup>, MJ Ryu<sup>1</sup>, SJ Kim<sup>1</sup>, YK Kim<sup>1</sup>, MJ Choi<sup>1</sup>, KS Kim<sup>1</sup>, JM Kim<sup>3</sup>, JW Kim<sup>4</sup>, YW Koh<sup>5</sup>, D-S Lim<sup>6</sup>, YS Jo<sup>1</sup> and M Shong<sup>1</sup>

The transcription coactivator Yes-associated protein 1 (YAP1) is regulated by the Hippo tumor suppressor pathway. However, the role of YAP1 in thyroid cancer, which is frequently associated with the *BRAF*<sup>V600E</sup> mutation, remains unknown. This study aimed to investigate the role of YAP1 in thyroid cancer. YAP1 was overexpressed in papillary (PTC) and anaplastic thyroid cancer, and nuclear YAP1 was more frequently detected in *BRAF*<sup>V600E</sup> (+) PTC. In the thyroid cancer cell lines TPC-1 and HTH7, which do not have the *BRAF*<sup>V600E</sup> mutation, YAP1 was cytosolic and inactive at high cell densities. In contrast, YAP1 was retained in the nucleus and its target genes were expressed in the thyroid cancer cells 8505C and K1, which harbor the *BRAF*<sup>V600E</sup> mutation, regardless of cell density. Furthermore, the nuclear activation of YAP1 in 8505C was not inhibited by *RAF* or *MEK* inhibitor. *In vitro* experiments, YAP1 silencing or overexpression affected migratory capacities of 8505C and TPC-1 cells. YAP1 knockdown resulted in marked decrease of tumor volume, invasion and distant metastasis in orthotopic tumor xenograft mouse models using the 8505C thyroid cancer cell line. Taken together, YAP1 is involved in the tumor progression of thyroid cancer and YAP1-mediated effects might not be affected by the currently used *RAF* kinase inhibitors.

*Oncogenesis* (2013) 2, e55; doi:10.1038/oncsis.2013.12; published online 15 July 2013

**Subject Categories:** Cellular oncogenes

**Keywords:** Yes-associated protein 1; proto-oncogene proteins B-Raf; thyroid neoplasm; orthotopic model; molecular targeted therapy; drug resistance

## INTRODUCTION

Thyroid cancer is the leading cause of morbidity and mortality for endocrine malignancies. Papillary thyroid cancer (PTC) is the most common thyroid cancer and is the result of the abnormal activation of the MEK/ERK signaling pathway.<sup>1</sup> The frequent genetic alterations, *RET/PTC* rearrangements, *Ras* mutations and *BRAF*<sup>V600E</sup> mutations in PTC uniformly result in the activation of the MEK/ERK pathway.<sup>2,3</sup> Of these genetic alterations, the *BRAF*<sup>V600E</sup> mutation has been identified as the most common genetic event related to PTC.<sup>4–6</sup> PTC appears to have a homogenous molecular signature in tumorigenesis compared with other human cancers,<sup>7</sup> but it has wide variability in clinical behaviors.<sup>8</sup> In fact, a subset of PTC is clinically aggressive and fatal due to the refractory nature of PTC to conventional radiation and drug treatment.<sup>9</sup> Although recent efforts to identify prognostic factors have helped to select patients who need appropriate treatment modalities, the current prognostic factors are not able to provide the molecular information that is potentially useful for prognostic evaluation and treatment of PTC.<sup>10,11</sup>

The Yes-associated protein 1 (YAP1) is a transcriptional coactivator that binds to TEA domain family members in mammals and acts as a downstream effector of the Hippo pathway.<sup>12</sup> The Hippo pathway is composed of the core kinases

Mst1/2 and Lats1/2 and two adapter proteins ww45 and Mats (Mob); these components are involved in tumorigenesis through a loss-of-function mechanism.<sup>13–15</sup> The loss of Hippo signaling components leads to the nuclear accumulation or aberrant activation of endogenous YAP1,<sup>16,17</sup> thus promoting the expression of genes controlling a cell-autonomous role in proliferation and cell-to-cell interactions. These effects were demonstrated through the increase of organ size in *Drosophila* and the increase of cell density in mouse embryos by YAP1 overexpression.<sup>12,18</sup> It has consistently been shown that the YAP1 protein is overexpressed in a wide spectrum of human cancer cell lines and primary tumors, including the lung, pancreatic, ovarian, hepatocellular, colorectal and prostate carcinomas.<sup>16,19–21</sup> More importantly, the upregulation of YAP1 expression is a prognostic marker in patients with nonsmall cell lung cancer and hepatocellular carcinoma.<sup>21,22</sup>

Raf-1 directly interacts with MST2 and thereby inhibits activating phosphorylation of MST2.<sup>23,24</sup> Additionally, MST2 mediates a signaling pathway controlled by RASSF1A, Raf-1 and Akt.<sup>25</sup> Furthermore, cooperative oncogenic Ras–Raf signaling is required to drive Yorkie/Scalloped-dependent epithelial tissue overgrowth in *Drosophila*.<sup>26</sup> However, the relationship between *BRAF*<sup>V600E</sup> and Hippo signaling has been barely investigated.

<sup>1</sup>Department of Internal Medicine, Research Center for Endocrine and Metabolic Disease, Chungnam National University School of Medicine, Daejeon, Korea; <sup>2</sup>Department of Pathology, Daejeon St Mary's Hospital, The Catholic University of Korea, Daejeon, Korea; <sup>3</sup>Department of Pathology, Chungnam National University Hospital, Daejeon, Korea; <sup>4</sup>Department of Otolaryngology-Head and Neck Surgery, Soon Chun Hyang University Hospital, Bucheon-Si, Korea; <sup>5</sup>Department of Otorhinolaryngology, Yonsei University College of Medicine, Seoul, Korea and <sup>6</sup>Department of Biological Sciences, Korea Advanced Institute of Science and Technology, Daejeon, Korea. Correspondence: Professor YS Jo, Department of Internal Medicine, Research Center for Endocrine and Metabolic Disease, Chungnam National University School of Medicine, 282 Munhwa-ro, Jung-gu, Daejeon 301-721, Korea or Professor M Shong, Department of Internal Medicine, Research Center for Endocrine and Metabolic Disease, Chungnam National University School of Medicine, 33 Munhwa-ro, Jung-gu, Daejeon 301-721, Korea.

E-mail: ysmrj@cnuh.co.kr or minhos@cnu.ac.kr

<sup>7</sup>These authors contributed equally to this work.

Received 22 November 2012; revised 20 April 2013; accepted 26 April 2013

Recently, we reported that the oncogenic effect of  $BRAF^{V600E}$  is associated with the inhibition of MST1, a master kinase of the Hippo tumor suppressor pathway, through direct interaction to repress the activity of the RASSF1A–MST1–FoxO3 pathway in  $BRAF^{V600E}$  tumors.<sup>27</sup> However, the YAP1 expression status and its role in human thyroid cancer were not demonstrated, and furthermore, the biological role of YAP1 in thyroid cancer in the context of  $BRAF^{V600E}$  activation remains to be determined. In this study, we show that YAP1 is frequently overexpressed in thyroid cancer and that its activation is related to the biological behavior of thyroid cancer.

## RESULTS

Nuclear expression of YAP1 is increased in human thyroid cancer samples

To investigate the expression pattern of YAP1 in thyroid cancer, we performed immunohistochemical (IHC) staining in paraffin-embedded tissues, including normal thyroid tissues (42 cases), PTC (131 cases), follicular adenoma (13 cases), follicular carcinoma (44 cases) and anaplastic thyroid cancer (9 cases). PTC and anaplastic thyroid cancer showed uniformly higher YAP1 staining scores compared with normal thyroid tissues, follicular adenoma

and follicular carcinoma (Supplementary Table 1). Furthermore, PTC demonstrated a statistically significant increased expression of YAP1 compared with normal thyroid tissue ( $P < 0.001$ , Figure 1a). Accordingly, the pattern of subcellular localization of YAP1 in PTC can be classified into three groups: group 1, 54 cases (41.2%) of PTC with nuclear YAP1; group 2, 48 cases (36.6%) with cytoplasmic YAP1; and group 3, 29 cases (22.1%) with nuclear and cytoplasmic YAP1 (Figure 1b). Interestingly, nuclear YAP1 showed a statistically significant association with the presence of extrathyroidal extension (Supplementary Table 2,  $P = 0.046$ ). Furthermore, when groups 1 and 3 were combined into one group, the statistical significance of the association of YAP1 with extrathyroidal extension was reinforced (Supplementary Table 3,  $P = 0.017$ ). Next, we compared the staining score and localization pattern of YAP1 according to the  $BRAF^{V600E}$  mutation status (Supplementary Table 4). The YAP1 staining scores of  $BRAF^{V600E}$ -positive PTC ( $BRAF^{V600E}$  (+) PTC) were statistically different from those of  $BRAF^{V600E}$ -negative PTC ( $BRAF^{V600E}$  (-) PTC,  $P = 0.031$ ). Remarkably, 88 cases (81.5%) of  $BRAF^{V600E}$  (+) PTC showed a strong staining intensity (score = 3), and 20 cases showed a moderate staining intensity. The subcellular localization of YAP1 in  $BRAF^{V600E}$  (+) PTC also differed from that of  $BRAF^{V600E}$  (-) PTC (Figure 1c,  $P < 0.001$ ). For  $BRAF^{V600E}$  (+) PTC, group 1 included 50

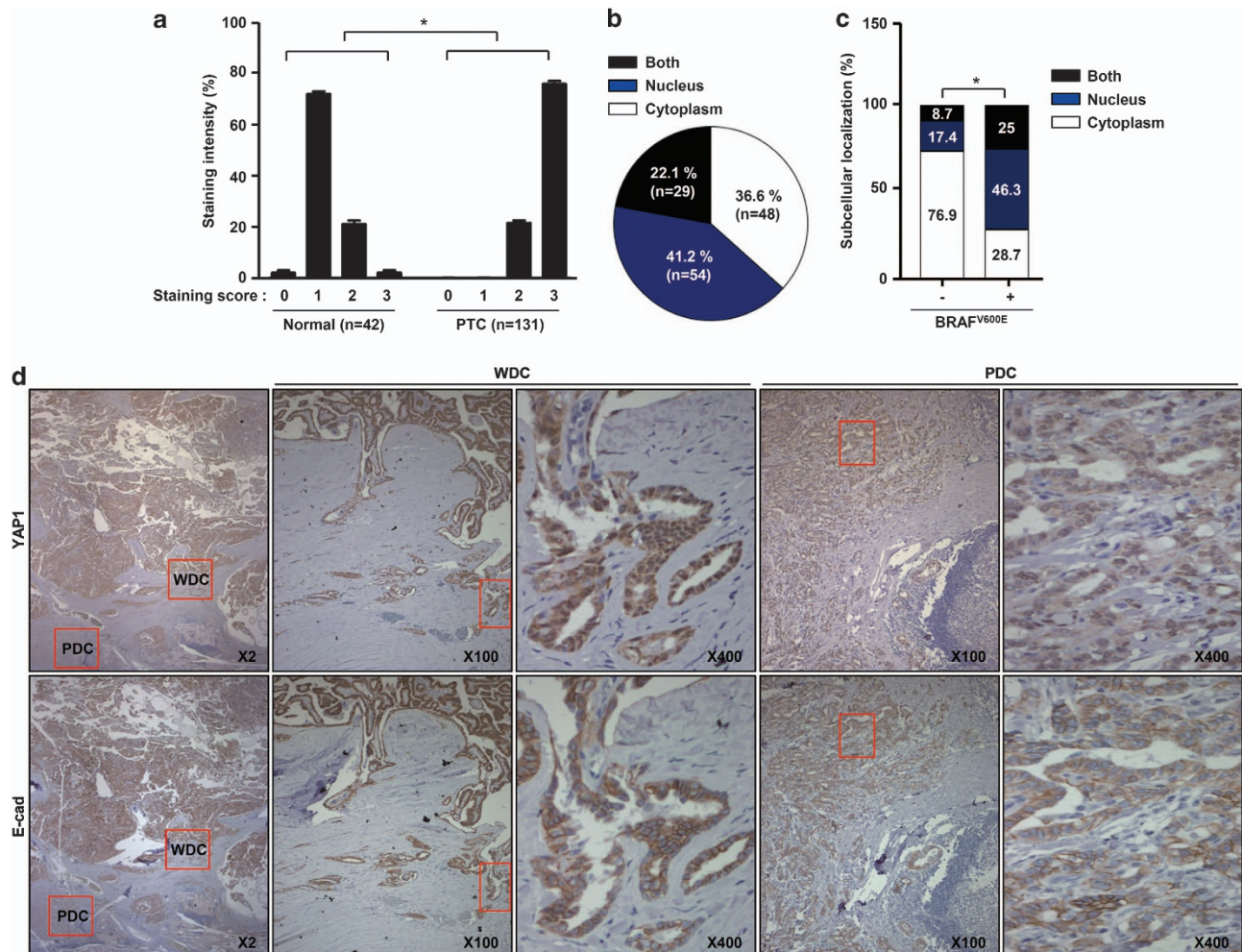


**Figure 1.** Nuclear overexpression of YAP1 in thyroid cancer. **(a)** Comparison of the YAP1 staining scores between normal thyroid tissue and PTC. The staining score was classified from 0 to 3 (see Materials and methods for a detailed description). **(b)** Subcellular localization of YAP1 in PTC. **(c)** Comparison of the subcellular localization of YAP1 according to the presence or absence of  $BRAF^{V600E}$  mutation. **(d)** The representative figures of YAP1 staining in  $BRAF^{V600E}$  (+) PTC composed of well-differentiated cell and poorly differentiated cell. Each upper figure and the corresponding lower figure are taken at the same sites from the tissue samples. Red boxes indicate the magnified area at the next high power field. \* $P$ -values are  $< 0.001$ .

cases (46.3%), group 2 consisted of 31 cases (28.7%) and group 3 included 27 cases (25%), whereas for *BRAF*<sup>V600E</sup> (-) PTC, group 1 contained 4 cases (17.4%), group 2 contained 17 cases (73.9%) and group 3 consisted of 2 cases (8.7%). Consistently, the 88 cases of *BRAF*<sup>V600E</sup> (+) PTC with strong staining intensities showed nuclear YAP1 localization: group 1, 39 cases (44.3%); group 2, 25 cases (28.4%); and group 3, 24 cases (27.3%). The analyses of the clinicopathological parameters showed that *BRAF*<sup>V600E</sup> (+) PTC was more frequently accompanied with extrathyroidal extension than *BRAF*<sup>V600E</sup> (-) PTC (Supplementary Table 5, *P* = 0.037). These observations suggested that the increased nuclear expression of YAP1 might promote the invasion of *BRAF*<sup>V600E</sup> (+) PTC into adjacent tissues.

E-cadherin, a member of the cadherin superfamily, ensures that cells within tissues are bound together. E-cadherin-mediated cell contact activates the Hippo pathway, resulting in the inhibition of cell proliferation with cytosolic translocation of YAP1.<sup>28</sup> However, YAP1 was persistently detected in the nucleus of *BRAF*<sup>V600E</sup> (+) PTC (Figure 1d upper row), whereas E-cadherin was easily detected in the cellular membrane, suggesting cell-to-cell adhesion (Figure 1d lower row).

Thus, these clinical and IHC data suggest that nuclear expression of YAP1 is able to affect the aggressiveness of *BRAF*<sup>V600E</sup> (+) PTC tumors, including extrathyroidal extension, independently from E-cadherin-mediated Hippo activation.

YAP1 is activated in the *BRAF*<sup>V600E</sup> (+) thyroid cancer cell lines, 8505C and K1, regardless of cell density

Based on the IHC results, we investigated whether nuclear YAP1 was consistently detected in thyroid cancer cell lines using immunofluorescent staining. Nuclear YAP1 (red) was easily detected in TPC-1, and HTH7 cells are *BRAF*<sup>V600E</sup> (-) thyroid cancer cell lines at low cell densities. However, the nuclear YAP1 signal disappeared while membrane  $\beta$ -catenin (green) was strongly expressed along with the cell membrane, suggesting cell-to-cell adhesion by high cell density (Figure 2a). The change of YAP1 transcriptional activity according to cell density was determined with real-time PCR for integrin beta 2 (*ITGB2*), which is known to be induced by YAP1 through a TEA domain-dependent manner.<sup>29</sup> As expected, *ITGB2* was remarkably decreased in TPC-1 cells at high cell densities (Supplementary Figure 1A). In contrast, nuclear YAP1 was persistently detected even at high cell densities in 8505C and K1 cells (*BRAF*<sup>V600E</sup> (+) thyroid cancer cell lines), suggesting that the nuclear localization of YAP1 is maintained regardless of cell density (Figure 2a). Interestingly, the induction of *ITGB2* in 8505C cells was markedly increased at high cell densities over that observed at low cell densities (Supplementary Figure 1B). At high cell densities, 8505C cells demonstrated a strong induction of *ITGB2* compared with TPC-1 cells (Figure 2c).

Next, we used the *BRAF*<sup>V600E</sup>- and *BRAF*<sup>WT</sup>-HEK293A cell lines to investigate the effect of the *BRAF*<sup>V600E</sup> mutation on the subcellular localization of YAP1. Although HEK293A cells are not derived from

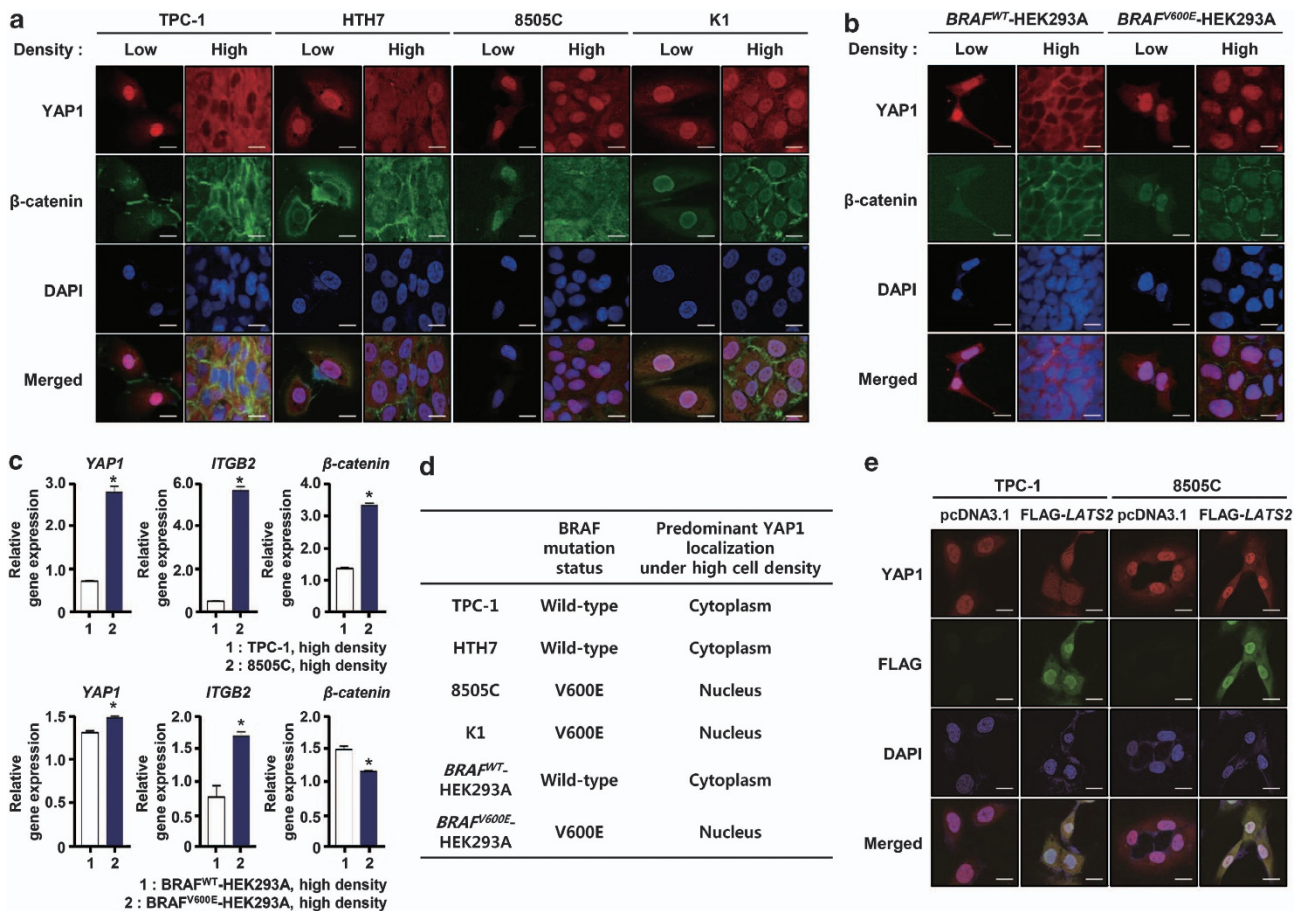


**Figure 2.** Persistent nuclear localization of YAP1 in thyroid cancer cells regardless of cell density. (a, b) Representative immunofluorescence figures demonstrate the subcellular localization of YAP1 in thyroid cancer cell lines (a), *BRAF*<sup>WT</sup>- and *BRAF*<sup>V600E</sup>-HEK293A cells (b). (c) Real-time PCR data showed mRNA expressions of YAP1, *ITGB2* and  $\beta$ -catenin in TPC-1, 8505C, *BRAF*<sup>WT</sup>- and *BRAF*<sup>V600E</sup>-HEK293A cells under high cell densities. \**P*-values are <0.05. Data represent the mean  $\pm$  s.d. of three independent experiments. (d) Summary of the subcellular localization of YAP1 in the cell lines used in this study. (e) Representative immunofluorescence images present the subcellular localization of YAP1 in TPC-1 and 8505C cells transfected with *LATS2* (1  $\mu$ g/well, 24 h).

the thyroid, the function of the tumor suppressor p53 is reduced in this cell line. This is similar to 8505C cell lines harboring an allelic deletion of the p53 gene<sup>30</sup> and to K1 cell lines with altered p53 function.<sup>31</sup> Therefore, we postulated that the effects of the *BRAF*<sup>V600E</sup> mutation are similar in the HEK293A, 8505C and K1 cell lines. *BRAF*<sup>WT</sup>-HEK293A showed nuclear YAP1 at low cell densities and cytoplasmic translocation of YAP1 at high cell densities (Figure 2b). In conjunction with the altered YAP1 localization, the expression of *ITGB2* was decreased by high cell density growth (Supplementary Figure 2A). In contrast, nuclear YAP1 was detected in both low and high cell densities, and persistent *ITGB2* induction was observed in *BRAF*<sup>V600E</sup>-HEK293A (Figure 2b and Supplementary Figure 2B). At high cell densities, *BRAF*<sup>V600E</sup>-HEK293A cells showed increased *ITGB2* expression compared with *BRAF*<sup>WT</sup>-HEK293A cells (Figure 2c). In summary, YAP1 was retained in the nucleus regardless of cell density in *BRAF*<sup>V600E</sup> (+) cell lines such as 8505C, K1 and *BRAF*<sup>V600E</sup>-HEK293A, whereas YAP1 shuttled between the nucleus and cytosol according to cell density in *BRAF*<sup>V600E</sup> (-) cell lines such as TPC-1, HTH7 and *BRAF*<sup>WT</sup>-HEK293A (Figure 2d).

To verify that the Hippo signaling pathway is altered in 8505C cells, we transfected TPC-1 and 8505C cells with *LATS2* kinase to inactivate YAP1 by enhancing its translocation from the nucleus to the cytosol. As shown in Figure 2e, *LATS2* initiated the cytosolic translocation of YAP1 in TPC-1 cells but not in 8505C cells. This

observation indicates that the Hippo signaling pathway may be suppressed in 8505C cells.

Nuclear YAP1 localization in thyroid cancer cells was not affected by RAF kinase inhibitors

The gain-of-function mutation of *BRAF*<sup>V600E</sup> induces a molecular structural change mimicking an active conformation.<sup>32</sup> Therefore, this mutation is associated with an increased kinase activity, which is related to cellular transformation in NIH3T3 cells.<sup>4</sup> On the basis of this finding, various kinase inhibitors have been developed and investigated in clinical trials.<sup>33,34</sup> Thus, we studied whether a broad-spectrum pan-RAF inhibitor (Sorafenib) and selective *BRAF*<sup>V600E</sup> inhibitor (PLX4720) were able to inhibit the nuclear localization of YAP1 in 8505C cells. In addition, we used MEK inhibitors such as PD98059 and U0126 to verify the role of MEK/ERK signaling in the regulation of YAP1 in *BRAF*<sup>V600E</sup> (+) 8505C cells. As shown in Figure 3a, nuclear YAP1 was detected in 8505C cells regardless of cell density, whereas  $\beta$ -catenin localized to the cell membrane at high cell densities. Interestingly, YAP1 was persistently detected in the nucleus after treatment with Sorafenib, PLX4720, PD98059 or U0126 at both low and high cell densities, even though these compounds effectively inhibited ERK phosphorylation (Figure 3b). These data suggest that *BRAF*<sup>V600E</sup> is

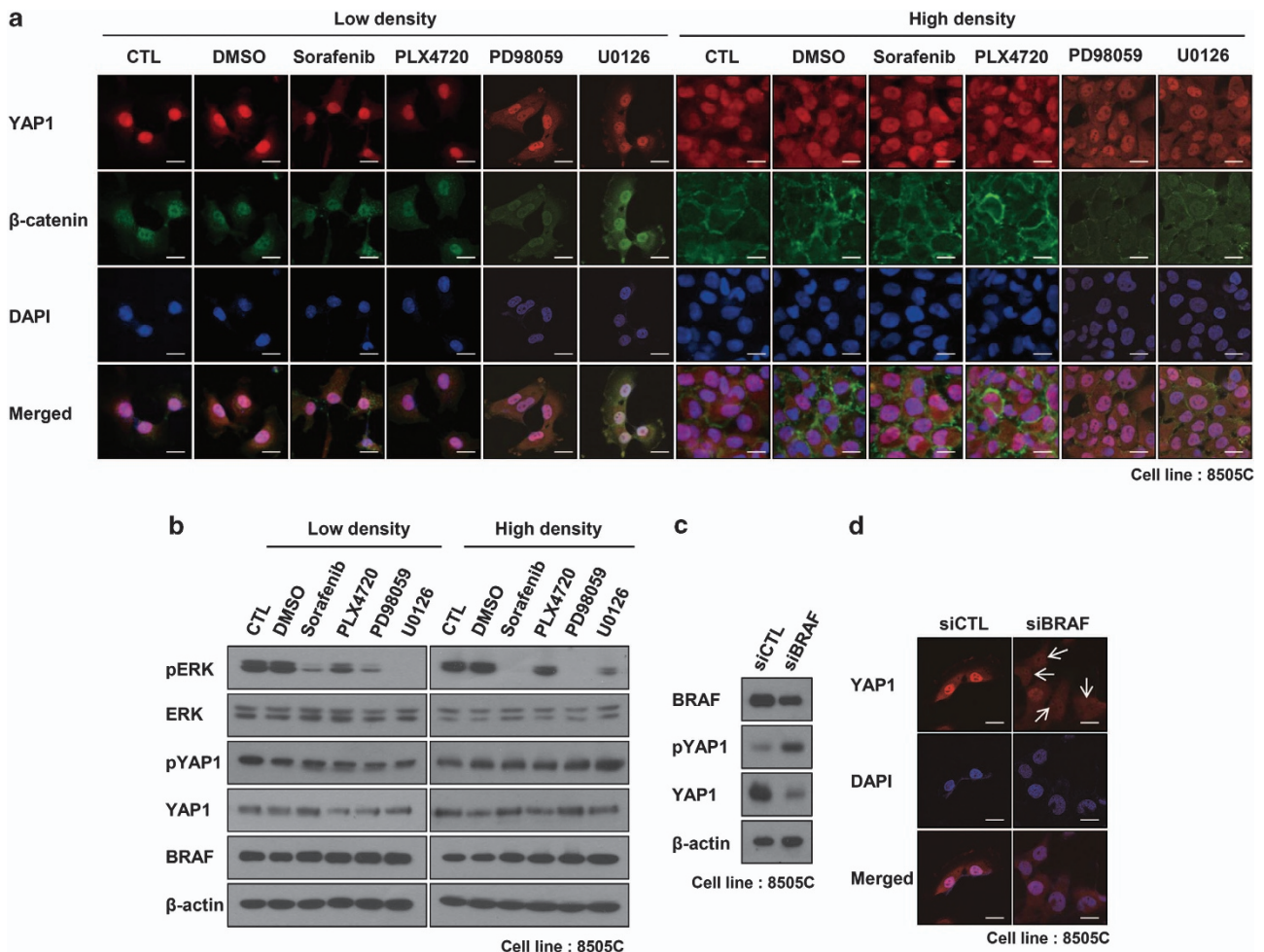


**Figure 3.** The effects of RAF kinase inhibitors on YAP1 transactivation by *BRAF*<sup>V600E</sup>-activated 8505C cells. **(a)** 8505C cells under low or high cell density were treated with Sorafenib (1  $\mu$ M), PLX4720 (1  $\mu$ M), PD98059 (50  $\mu$ M) or U0126 (1  $\mu$ M) for 2 h.  $\beta$ -Catenin was used as a marker of cell-to-cell contact, and nuclear staining was performed using 4, 6-diamidino-2-phenylindole (DAPI). **(b)** The results of western blot analyses to verify the effect of ERK or YAP1 S127 phosphorylation by inhibitors. **(c, d)** The results of western blot analyses and immunofluorescence staining to present the effect of YAP1 activation by BRAF silencing in 8505C cells. CTL, control; DMSO, dimethyl sulfoxide.

able to retain nuclear YAP1 in the 8505C cells, but this retention is not dependent on the kinase activities of the RAF and MEK/ERK signaling pathways. In contrast, the silencing of *BRAF*<sup>V600E</sup> by transfecting siBRAF resulted in an increase in the inactivating phosphorylation (S127) and cytosolic translocation of YAP1 (Figures 3c and d). Thus, nuclear YAP1 is associated with the *BRAF*<sup>V600E</sup> mutation but is not related to RAF kinase or MEK/ERK activity.

**YAP1 promotes the migration of thyroid cancer cells *in vitro***

As YAP1 was retained in the nucleus in 8505C cells regardless of cell density, we investigated the effect of YAP1 on tumor behavior in these cells. To perform the *in vitro* cell viability assay, we silenced YAP1 expression in 8505C cells (shYAP1-8505C) using a shYAP1 plasmid-based RNA interfering technique (Supplementary Figure 3A), and observed that shYAP1-8505C demonstrated no differences in cell viability compared with control small hairpin RNA-transfected 8505C cells (shCTL-8505C) (Supplementary Figure 3B). However, in the scratch assays performed to determine whether YAP1 affected the migration ability of *BRAF*<sup>V600E</sup>-activated 8505C cells, shYAP1-8505C showed a remarkably lower migration rate compared with shCTL-8505C ( $46.2 \pm 7.4\%$  vs  $22.9 \pm 3.9\%$ , respectively,  $P=0.009$ , Figures 4a and b). To verify the role of YAP1 in thyroid cancer cell migration, we transfected TPC-1 cells with YAP1 and YAP1 S127A vectors. The YAP1 S127A mutant is

independent from LATS1/2 and maintains a constitutive level of transactivation.<sup>12</sup> Wild-type YAP1-transfected TPC-1 cells showed a higher migration rate than control TPC-1 cells ( $75.6 \pm 5.6\%$  vs  $67.6 \pm 3.5\%$ , respectively,  $P=0.028$ ). Moreover, YAP1 S127A-transfected TPC-1 cells showed the highest migration rate (YAP1 S127A vs control;  $97.1 \pm 0.6\%$  vs  $67.6 \pm 3.5\%$ ,  $P=0.009$ , YAP1 S127A vs WT;  $P=0.05$ ; Figures 4c and d). These *in vitro* experiments demonstrate that YAP1 has a role in the invasion of thyroid cancer cells in agreement with our human clinicopathological analysis.

Silencing of YAP1 reduced tumor size and decreased expression of genes related to tumor aggressiveness in an orthotopic thyroid cancer model

On the basis of the results from the clinical and *in vitro* data, we decided to perform phenotype analyses using an orthotopic thyroid cancer model to demonstrate that YAP1 promotes the invasion of *BRAF*<sup>V600E</sup>-activated 8505C cells *in vivo*. Interestingly, 4 weeks after tumor cell injection (shYAP1-8505C or shCTL-8505C), a gross inspection of the thyroid gland from shCTL-8505C-injected mice (shCOM) demonstrated markedly enlarged thyroid tumors accompanied with peritumoral bleeding (Figure 5a). The estimated tumor volume of shCOM was significantly larger than that of shYAP1-8505C-injected mice (shYAM) ( $57.7 \pm 20.1$  vs  $3.3 \pm 2.5$  cm<sup>3</sup>, respectively,  $P=0.009$ , Figure 5b). The use of

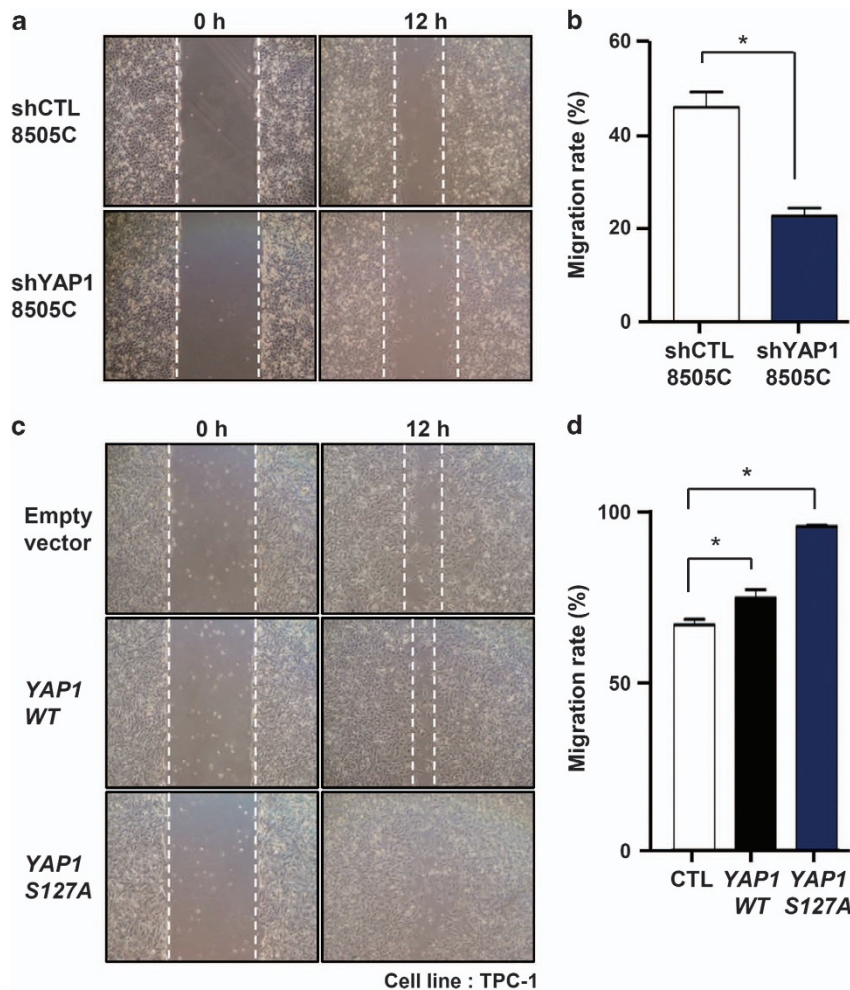


**Figure 4.** The migration ability promoted by YAP1 in thyroid cancer cell lines. (a, b) The scratch assays were performed using shCTL-8505C and shYAP1-8505C. At 12 h after scratching, the migration rates were calculated (the distance from the right to left border at 12 h divided by the distance from the right to left border at the start time). (c, d) The scratch assays were performed using TPC-1 cells transfected with empty vector, wild-type YAP1 (YAP1 WT) or YAP1 S127A. At 12 h after scratching, the migration rates were calculated. \**P*-values are <0.01. Data represent the mean ± s.d. of three independent experiments.

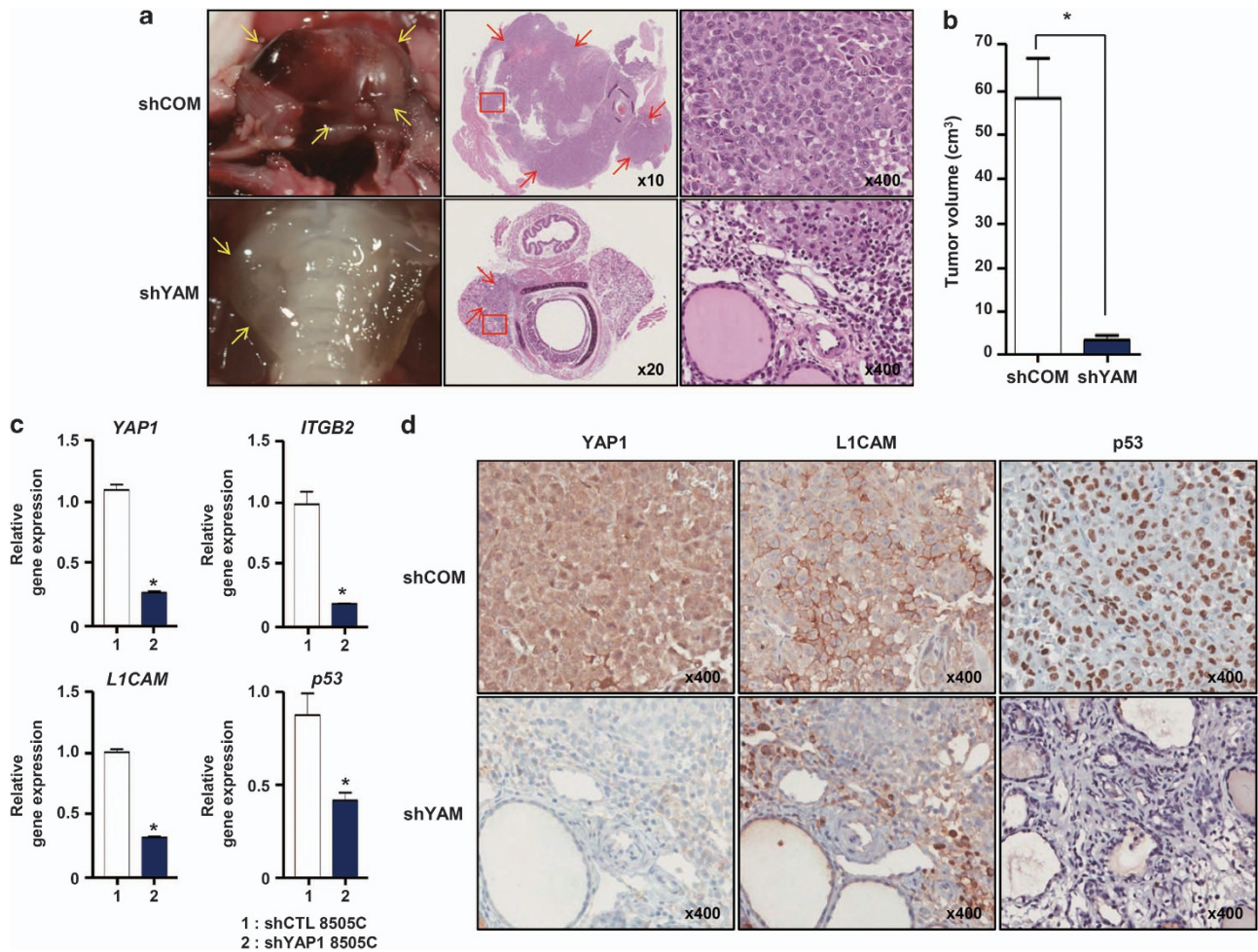


**Figure 5.** The relation of YAP1 to molecular markers indicating tumor aggressiveness in *BRAF*<sup>V600E</sup>-activated 8505C cells injected thyroid cancer. **(a)** Gross and microscopic inspection of thyroids from shCOM and shYAM. Arrows indicate thyroid tumors, and the red boxes indicate the magnified areas at the next high power field. **(b)** The comparison of tumor volumes from shCOM ( $n = 6$ ) and shYAM ( $n = 6$ ). **(c)** Real-time PCR data demonstrating the effect of YAP1 silencing in 8505C cells.  $P$ -values are  $< 0.01$ . Data represent the mean  $\pm$  s.d. **(d)** IHC staining to detect YAP1, L1CAM and p53 in thyroids from shCOM and shYAM. The red boxes indicate the magnified areas at the next high power field.

orthotopic tumor models offers a similar microenvironment, cell growth and metastatic pattern to that of human cancer compared with subcutaneous tumor models.<sup>35</sup> Consequently, the small tumor volume of shYAM in this model indicates that YAP1 might be related to the tumor aggressiveness of thyroid cancer, as shown by the *in vitro* experiments.

Supporting the histological observations, the orthotopic model showed a differential expression pattern of the ITGB2, L1 cell adhesion molecule (L1CAM) and p53 between shCOM and shYAM (Figure 5c). L1CAM was identified in the nervous system as a member of the immunoglobulin superfamily. However, recent studies reported that L1CAM is detected at the cell membrane of invasive front of tumors, suggesting that L1CAM is strongly associated with tumor invasion and progression.<sup>36</sup> In fact, L1CAM and YAP1 have been postulated as novel targets of Wnt/ $\beta$ -catenin signaling.<sup>37,38</sup> Furthermore, our group has recently reported that L1CAM has an important role in determining tumor behavior and chemosensitivity in anaplastic thyroid cancers.<sup>39</sup> On the basis of these findings, we postulated that L1CAM and YAP1 might have synergistic effects on epithelial to mesenchymal changes, resulting in the invasion of adjacent normal tissues. Compatible with our idea, IHC staining demonstrated membrane localization of L1CAM in shCOM tumor cells. However, the expression level of L1CAM was remarkably decreased and the subcellular localization of L1CAM was

mainly in the cytoplasm rather than membrane-localized in shYAM thyroid tumors (Figure 5d). As 8505C cells have a mutated p53, the expression of p53 represents the dedifferentiation of the tumor cells.<sup>30</sup> In our orthotopic model, p53 expression was increased in tumors from shCOM compared with shYAM (Figures 5c and d).

Thus, orthotopic tumors derived from shYAP1-8505C cells were small and the expression of L1CAM and p53 was reduced, which suggests that YAP1 may affect the aggressiveness of thyroid tumors.

Silencing of YAP1 resulted in decreased tumor invasion and distant metastasis in an orthotopic thyroid cancer model

Next, we examined the invasive tumor front adjacent tissue and analyzed the metastatic foci in the lungs from shCOM and shYAM. shCOM showed tumor cells that had extensively penetrated into the tracheal cartilage, resulting in the destruction of the bronchial epithelium and finally inducing airway distortion. Tumor cells of shCOM also strikingly infiltrated into the esophageal submucosa, resulting in the destruction of the esophageal muscle, which was replaced by tumor cells in the invasion area (Figure 6a and Supplementary Figure 4A). In contrast, shYAM showed minimal invasion along the trachea, did not infiltrate into the submucosal glands and did not

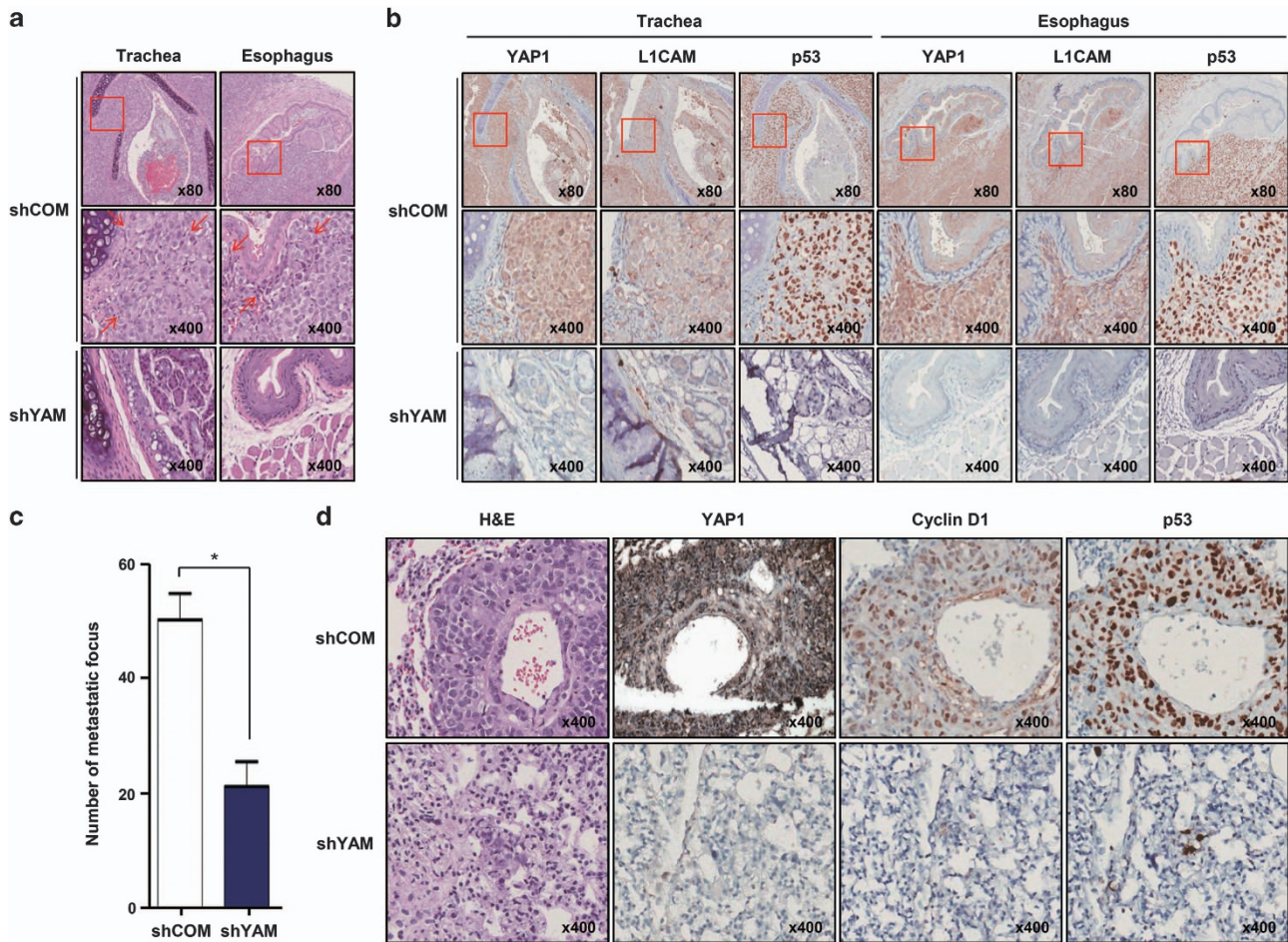


**Figure 6.** The effect of YAP1 on tumor invasion and metastasis into adjacent tissues in *BRAF<sup>V600E</sup>*-activated 8505C cells injected thyroid cancer. **(a)** The comparison of adjacent tissue invasion, such as esophagus and trachea, between shCOM and shYAM. Arrows indicate the invasive front of the thyroid tumors, and the red boxes indicate the magnified areas at high power fields. **(b)** IHC staining of the magnified areas in **a** to detect YAP1, L1CAM and p53 in the invasive fronts from shCOM and shYAM. **(c)** The comparison of the number of metastatic foci between shCOM and shYAM (see Materials and methods for detail description). **(d)** IHC staining of magnified areas in Supplementary Figure 5 to detect YAP1, L1CAM and cyclin D1 in the lungs from shCOM and shYAM.

affect airway patency. shYAM also demonstrated an intact esophageal muscle (Figure 6a, shYAM). As expected, the invasive front of the tumors from shCOM showed strong membranous L1CAM expression (Figure 6b and Supplementary Figure 4B). However, tumor cells of shYAM had lower expression levels of L1CAM in the invasive front (Figure 6b). Consistent with the results presented in Figure 5, p53 expression was markedly increased in tumors from shCOM (Figure 6b).

To examine the role of YAP1 in tumor metastasis, we characterized the metastatic foci in the lungs from shCOM and shYAM. Upon gross inspection of the lungs, we found metastatic foci in the lung from shCOM (Supplementary Figure 5). Microscopic metastatic foci were detected in animals for both tumor groups; however, when we counted and statistically analyzed the data, the number of metastatic foci in shCOM was markedly higher than that in shYAM ( $51.4 \pm 4.7$  vs  $21.8 \pm 4.4$ , respectively,  $P=0.009$ , Figure 6c). Furthermore, the IHC study showed that cyclin D1 and p53 were remarkably increased in the metastatic foci of shCOM compared with shYAM (Figure 6d).

In summary, tumors derived from shYAP1-8505C cells were less invasive and had fewer metastatic foci than the tumors derived from shCTL-8505C cells. Taken together with the results of the IHC study, these histological features suggest that YAP1 may have

roles in tumor invasion and in distant metastasis in patients with thyroid cancer.

## DISCUSSION

In this study, we used human samples, cell lines and orthotopic models to investigate the role of YAP1 in thyroid cancer (Supplementary Figure 6). We demonstrated that YAP1 is retained in the nucleus in human thyroid cancer even when E-cadherin-mediated activation of Hippo might be functional. Furthermore, nuclear localization of YAP1 was positively associated with extrathyroidal extension in cells harboring the *BRAF<sup>V600E</sup>* mutation. In support of our clinical data, immunofluorescent staining consistently demonstrated that YAP1 is retained in the nucleus in 8505C and K1 cells, which harbor the *BRAF<sup>V600E</sup>* mutation, at high density. The Hippo pathway is an essential process for the growth regulatory network of epithelial tissues to inhibit outgrowth of organ size<sup>40–42</sup> and maintain the apico-basal cell polarity.<sup>43,44</sup> In this context, cell adhesion and cell junction proteins induce the Hippo pathway to inactivate YAP1 via LATS1/2 and turnoff YAP1-dependent transcriptional output.<sup>15</sup> In *Drosophila*, the binding of Fat, a protocadherin, with Ds leads to the recognition of cell-to-cell contact, which may be the initial

step of Hippo activation promoted by the Ex-Mer-Kibra complex.<sup>45,46</sup> In mammals, although the exact function of the Fat and Ex homologs are not verified, Mer and RASSF, members of the Ras effector protein family, activate Mst1/2, suggesting that the sensors to detect cell-to-cell contact may be working to activate the Hippo pathway.<sup>47,48</sup> Thus, our clinical and *in vitro* data suggest that nuclear retention of YAP1 in thyroid cancer might be a signature event in the escape from organ size control systems. Supporting our hypothesis, the real-time PCR data showed that *ITGB2*, a YAP1-inducible gene, was markedly increased in 8505C cells and in *BRAF*<sup>V600E</sup>-HEK293A cells even under high cell density. Moreover, shYAP1-8505C cells also showed decreased mRNA levels of *ITGB2*. In fact, YAP1 potently induces *ITGB2* expression through TEA domain family transcriptional factors,<sup>29</sup> promoting the epithelial-mesenchymal transition of tumor cells.<sup>49,50</sup>

Interestingly, when the TPC-1 and 8505C cell lines were transfected with *LATS2*, which leads to inhibitory phosphorylation (S127) of YAP1, and can thereby promote the translocation of YAP1 from the nucleus to the cytoplasm, YAP1 was cytosolic in TPC-1 cells, whereas it was retained in the nucleus in 8505C cells. This suggests that Hippo signaling might be aberrant in 8505C cells, which harbor the *BRAF*<sup>V600E</sup> mutation. In addition to Mst1/2-Lats1/2-mediated YAP1 regulation, YAP1 is regulated by cross-talk with angiomin/angiomin-like 1<sup>51,52</sup> or mechanical cues delivered by Rho and stress fibers.<sup>53</sup> Therefore, we may suspect that *BRAF*<sup>V600E</sup> promotes YAP1 transactivation via the regulation of these factors. However, the relationship of *BRAF*<sup>V600E</sup> with angiomin/angiomin-like 1 has not been clarified *in vitro* or *in vivo*. Furthermore, maintenance of actin stress fibers in fibroblasts by Rho-associated coiled-coil-containing protein kinase II is regulated by BRAF in a MEK-dependent manner.<sup>54</sup> However, treatment with the pan-RAF kinase inhibitor (Sorafenib), the *BRAF*<sup>V600E</sup> kinase inhibitor (PLX4720) or MEK inhibitors such as PD98059 and U0126 did not abolish the nuclear accumulation of YAP1 in *BRAF*<sup>V600E</sup> (+) 8505C cells. In contrast, *BRAF*<sup>V600E</sup> silencing promoted S127 phosphorylation and the cytosolic localization of YAP1. Therefore, a possible regulatory mechanism of YAP1 via *BRAF*<sup>V600E</sup> is that the Hippo signal is directly inactivated by *BRAF*<sup>V600E</sup> through the MST1/2 interaction independently from the *BRAF*<sup>V600E</sup> kinase activity, which our group has previously reported.<sup>27</sup>

Additionally, our study demonstrated that YAP1 was clearly associated with tumor invasion *in vitro* and *in vivo*. Based on the results of the *in vitro* cell viability assay, the cell viability of the two cell lines, shCTL-8505C and shYAP1-8505C, was identical. However, a scratch assay suggested that YAP1 deletion or overexpression affected cell mobility in 8505C and TPC-1 thyroid cancer cell lines, respectively, as seen in other models, such as in G $\beta$  signaling or 15-hydroxyprostaglandin dehydrogenase.<sup>55,56</sup> Furthermore, an orthotopic mouse model demonstrated that the deletion of YAP1 modified tumor behaviors and generated a more favorable outcome. As discussed, YAP1 inactivation by the Hippo pathway might have a pivotal role in the control of cell proliferation, and may thus prevent tumorigenesis, which was strongly supported by the liver-specific ablation of ww45 (adapter for Hippo kinase).<sup>57</sup> From this point of view, previous studies have reported that overexpression of YAP1 was highly associated with poor prognosis in patients with hepatocellular carcinoma, ovarian serous tumors or gastric cancer.<sup>19–21</sup> However, the multiple steps of carcinogenesis, such as proliferation, invasion and even metastasis, have not been observed in a single YAP1 animal model to understand how it contributes to cancer cell biology at each step. Remarkably, increased expression of L1CAM was detected in primary sites of shCOM, and mutated p53, as a hallmark of undifferentiated carcinoma, was increased in the primary sites and metastatic lesions of shCOM compared with shYAM. Furthermore, nuclear cyclin D1 was only observed in the metastatic lesions of shCOM. These microscopic observations and

IHC data suggested that the deletion of YAP1 affected the molecular signatures required by individual carcinogenic steps, such as L1CAM for invasion, p53 for dedifferentiation and cyclin D1 for the establishment of metastasis.<sup>58</sup> Thus, thyroid cancers may require YAP1 activity to gain the aggressive features necessary to invade adjacent tissue and metastasize to distant organs *in vivo*.

In conclusion, nuclear YAP1 would appear to be associated with the extrathyroidal extension of thyroid cancer in patients with *BRAF*<sup>V600E</sup> (+) PTC and with aggressive features such as migration, local invasion and distant metastasis in *in vitro* and *in vivo* models. Furthermore, the nuclear activation of YAP1 was maintained in 8505C and K1 cells, and resistant to RAF, *BRAF*<sup>V600E</sup> and MEK inhibitors. Therefore, the YAP1 silencing or inhibition might be a future therapeutic target in aggressive thyroid cancers.

## MATERIALS AND METHODS

### Selection of patients and analysis of clinicopathological data

Thyroid tissue specimens were obtained from 197 patients who underwent surgery from 2004 to 2005 at the Center for Endocrine Surgery, Chungnam National University Hospital, Daejeon, Korea. Microscopically normal thyroid tissues were obtained from patients who underwent thyroidectomy because they had benign thyroid diseases (7 cases of follicular adenoma and 35 cases of nodular hyperplasia). Patient information and clinicopathological parameters were analyzed. For staging PTC samples, the Tumor Node Metastasis classification of the International Union Against Cancer (UICC) was used. All protocols were approved by the institutional review board.

### DNA isolation and pyrosequencing

Genomic DNA from paraffin-embedded thyroid tissue specimens consisting of more than 90% tumor cells was prepared from five 10- $\mu$ m-thick sections after microdissection. After the sections were deparaffinized, genomic DNA was isolated using the EZ1 DNA Tissue Kit (Qiagen, Chatsworth, CA, USA). Genomic DNA amplification, the purification of the amplified products and pyrosequencing were performed as previously described.<sup>59</sup>

### Cell lines

HEK293A and 8505C cells were purchased from the American Type Culture Collection (ATCC, Manassas, VA, USA). K1 cells were obtained from the European Collection for Cell Cultures (ECACC, Salisbury, UK). HTH7 and TPC-1 cells were provided by Dr M Santoro (Università di Napoli Federico II, Naples, Italy) and Dr Masahide Takahashi (Nagoya University, Nagoya, Japan), respectively. HEK293 cell lines stably expressing *BRAF*<sup>V600E</sup> or wild-type *BRAF* (*BRAF*<sup>V600E</sup>-HEK293A and *BRAF*<sup>WT</sup>-HEK293A, respectively) were generated using the ViraPower lentiviral expression system (Invitrogen, Carlsbad, CA, USA). The 8505C YAP1 silenced (shYAP1-8505C) and control small hairpin RNA (shCTL-8505C) cell lines were generated using MISSION small hairpin RNA lentiviral transduction particles (Sigma-Aldrich, St Louis, MO, USA).

### Cell culture and transfection

TPC-1, HTH7 and K1 cells were cultured in Dulbecco's modified Eagle medium with 10% fetal bovine serum. 8505C cells were cultured in RPMI1640. TPC-1 and 8505C cells were grown in six-well plates and transfected with FLAG-*LATS2* (1  $\mu$ g/well) for 24 h using Lipofectamine PLUS (Invitrogen). 8505C cells were transfected with 20 pmol Stealth siRNA or siBRAF (Invitrogen) oligomers in 50  $\mu$ l Opti-MEM I using Lipofectamine RNAiMAX (Invitrogen). All experiments were performed in duplicate and were repeated at least three times.

### Immunohistochemistry

Paraffin-embedded tissue samples were prepared for IHC staining using a standard protocol.<sup>17</sup> The primary antibodies used in this study were anti-YAP1 (Santa Cruz Biotechnology, Santa Cruz, CA, USA), anti-E-cadherin (Cell Signaling Technology, Beverly, MA, USA), anti-L1CAM (Abcam, Cambridge, UK), anti-p53 (Dako, Copenhagen, Denmark) and anti-cyclin D1 (Dako). Negative controls were incubated with phosphate-buffered saline instead

of a primary antibody, and no positive staining was observed. In addition, positive controls were performed with sections of lung squamous cell carcinoma and stained for YAP1, p53 and cyclin D1, as well as nerve bundles for L1CAM and breast ductal carcinoma for E-cadherin. To classify the IHC results for the human samples, we used the following scoring system: 0, no staining; 1, weak staining in the focal area; 2, moderate staining in most cells; and 3, strong staining in most cells. The IHC results were evaluated by two independent pathologists (JUL and JMK).

#### RNA isolation and real-time PCR

RNA isolation and real-time PCR were performed according to the manufacturer's protocol. Briefly, total RNA was extracted using Trizol (Invitrogen), and complementary DNA (cDNA) was prepared from total RNA using M-MLV Reverse Transcriptase (Invitrogen) and oligo-dT primers (Promega, Madison, WI, USA). Real-time PCR was performed using cDNA, QuantiTect SYBR Green PCR Master Mix (Qiagen, Valencia, CA, USA) and specific primers (Supplementary Table 6). The relative expression was calculated using the Rotor-Gene 6000 real-time rotary analyzer software (Version 1.7, Corbett Life Science, Sydney, Australia). Real-time PCR experiments were performed in triplicate and were repeated three times.

#### Immunofluorescence staining

The cells were plated on coverslips in six-well plates. Low confluence cells were plated at  $1 \times 10^5$  cells/well, and high confluence cells were plated at  $5 \times 10^5$  cells/well. After 3 days, the cells were fixed and permeabilized using conventional methods. Then, the cells were incubated with anti-YAP1 (Santa Cruz Biotechnology) and anti- $\beta$ -catenin (Santa Cruz Biotechnology) antibodies at a 1:100 dilution in 3% bovine serum albumin for 24 h at 4 °C. After washing, cells were incubated with Cy2-conjugated pure goat anti-mouse and TRITC (Rhodamine)-conjugated pure goat anti-rabbit (Jackson ImmunoResearch Laboratories Inc., West Grove, PA, USA). Nuclei were stained using 4, 6-diamidino-2-phenylindole (DAPI, Sigma-Aldrich). After washing the cells, cells on the coverslips were mounted on glass slides using mounting medium (Sigma-Aldrich) and observed using a laser-scanning confocal microscope (Olympus Corp., Tokyo, Japan). All experiments were performed in duplicate and were repeated at least five times.

#### Cell viability assay

shCTL-8505C and shYAP1-8505C cells were plated in 96-well plates at  $1 \times 10^2$  cells/well in 200  $\mu$ l of RPMI1640. At the indicated times, an MTT solution (Sigma-Aldrich) was added to the plated cells. During 96 h, we measured the absorbance at 595 nm using an E max precision microplate reader (Molecular Devices, Sunnyvale, CA, USA). Experiments were performed in triplicate and were repeated at least three times.

#### Immunoblot analysis

Cells were lysed in lysis buffer, and the cell lysates were separated using SDS-polyacrylamide gel electrophoresis. After the proteins were transferred to a nitrocellulose (NS) membrane (Amersham Biosciences, Freiburg, Germany), the membranes were blocked with 5% skim milk and incubated with the indicated primary antibodies overnight at 4 °C, and with the indicated secondary antibodies for 1 h at room temperature. The immunoreactive bands were developed using peroxidase-conjugated secondary antibodies (Phototope-HRP Western Blot Detection Kit, New England Biolabs, Beverly, MA, USA).

#### Scratch assay

shCTL-8505C and shYAP1-8505C cells were plated in six-well plates at  $5 \times 10^5$  cells/well. After 3 days, the cell surface in three places were scratched using a p200 pipette tip. Additionally, TPC-1 cells were plated in six-well plates and after 24 h, were transfected with pCMV-HA-YAP1 or pCMV-HA-YAP1 S127A using Lipofectamine PLUS (Invitrogen). Next, the cell surface was scratched using a p200 pipette tip after 2 days. The cells were observed after 12 h using an Olympus IX71 microscope (Olympus). Human cDNAs for YAP1 were cloned into pDK-Flag2 or pCMV-HA (HA, hemagglutinin), which had been modified from pcDNA3.1 or pcDNA3 (Invitrogen). Site-directed PCR mutagenesis was used to introduce the missense change S127A into the YAP1 sequence.<sup>40</sup> Migration rates were calculated using the following equation: (full-length-scratched-length)/full-length  $\times$  100. Image analysis was performed using the ImageJ v1.42q software (National Institutes of Health, USA). All experiments were performed in triplicate and were repeated two times.

#### Orthotopic mouse model of thyroid cancer

Eight-week-old male nude mice were purchased from Japan SLC Inc. Before injection of the cell lines into the mice, shCTL-8505C and shYAP1-8505C cells were diluted to  $1 \times 10^5$  cells/ $\mu$ l in RPMI1640. Each cell line was injected into six mice. To inject 5  $\mu$ l ( $5 \times 10^5$ ) of cells into the right thyroid, a 33-gauge beveled needle (World Precision Instruments Inc., Sarasota, FL, USA) and a 100- $\mu$ l nanofil syringe (World Precision Instruments Inc.) were used. The mice were killed 4 weeks after injection, and tumor volumes were calculated using the established equation: length  $\times$  width<sup>2</sup>  $\times$  0.5.<sup>60</sup> Thyroid glands and lungs from the mice were placed in formalin solution, and each tissue was embedded in paraffin. The metastatic foci were counted on 100 randomly selected high power fields in each experimental group. All animal procedures were performed under the guidelines of the Institutional Animal Care and Use Committee of the Chungnam National University School of Medicine.

#### Statistical analysis

Group comparisons of categorical variables were evaluated using the  $\chi^2$  test or linear-by-linear association. Comparisons of average means were performed with the independent sample *t*-test, one-way analysis of variance or Mann-Whitney *U*-test. All reported *P*-values are two sided. Analyses were performed using SPSS Versions 18.0 for Windows.

#### CONFLICT OF INTEREST

The authors declare no conflict of interest.

#### ACKNOWLEDGEMENTS

Sorafenib and PLX4720 were kindly provided by Bayer Schering Pharma AG and Plexicon Inc. This work was supported in part by the second phase of the Brain Korea 21 program of the Ministry of Education and by the Korea Healthcare Technology R&D Project, Ministry for Health, Welfare and Family Affairs, Republic of Korea (A100588). SEL, MJR and YSJ were supported by NRF/MEST (No. 2011-0005834, 2012R1A2A2A01014672).

#### REFERENCES

- 1 Cohen Y, Xing M, Mambo E, Guo Z, Wu G, Trink B *et al*. BRAF mutation in papillary thyroid carcinoma. *J Natl Cancer Inst* 2003; **95**: 625–627.
- 2 Kondo T, Ezzat S, Asa SL. Pathogenetic mechanisms in thyroid follicular-cell neoplasia. *Nat Rev Cancer* 2006; **6**: 292–306.
- 3 Pratilas CA, Taylor BS, Ye Q, Viale A, Sander C, Solit DB *et al*. (V600E)BRAF is associated with disabled feedback inhibition of RAF-MEK signaling and elevated transcriptional output of the pathway. *Proc Natl Acad Sci USA* 2009; **106**: 4519–4524.
- 4 Davies H, Bignell GR, Cox C, Stephens P, Edkins S, Clegg S *et al*. Mutations of the BRAF gene in human cancer. *Nature* 2002; **417**: 949–954.
- 5 Kimura ET, Nikiforova MN, Zhu Z, Knauf JA, Nikiforov YE, Fagin JA. High prevalence of BRAF mutations in thyroid cancer: genetic evidence for constitutive activation of the RET/PTC-RAS-BRAF signaling pathway in papillary thyroid carcinoma. *Cancer Res* 2003; **63**: 1454–1457.
- 6 Puxeddu E, Durante C, Avenia N, Filetti S, Russo D. Clinical implications of BRAF mutation in thyroid carcinoma. *Trends Endocrinol Metab* 2008; **19**: 138–145.
- 7 Soares P, Trovisco V, Rocha AS, Lima J, Castro P, Preto A *et al*. BRAF mutations and RET/PTC rearrangements are alternative events in the etiopathogenesis of PTC. *Oncogene* 2003; **22**: 4578–4580.
- 8 Nikiforova MN, Kimura ET, Gandhi M, Biddinger PW, Knauf JA, Basolo F *et al*. BRAF mutations in thyroid tumors are restricted to papillary carcinomas and anaplastic or poorly differentiated carcinomas arising from papillary carcinomas. *J Clin Endocrinol Metab* 2003; **88**: 5399–5404.
- 9 Hong DS, Cabanillas ME, Wheler J, Naing A, Tsimberidou AM, Ye L *et al*. Inhibition of the Ras/Raf/MEK/ERK and RET kinase pathways with the combination of the multikinase inhibitor sorafenib and the farnesyltransferase inhibitor tipifarnib in medullary and differentiated thyroid malignancies. *J Clin Endocrinol Metab* 2011; **96**: 997–1005.
- 10 Nikiforov YE, Nikiforova MN. Molecular genetics and diagnosis of thyroid cancer. *Nat Rev Endocrinol* 2011; **7**: 569–580.
- 11 Cooper DS, Doherty GM, Haugen BR, Kloos RT, Lee SL, Mandel SJ *et al*. Revised American Thyroid Association management guidelines for patients with thyroid nodules and differentiated thyroid cancer. *Thyroid* 2009; **19**: 1167–1214.

- 12 Ota M, Sasaki H. Mammalian Tead proteins regulate cell proliferation and contact inhibition as transcriptional mediators of Hippo signaling. *Development* 2008; **135**: 4059–4069.
- 13 Saucedo LJ, Edgar BA. Filling out the Hippo pathway. *Nat Rev Mol Cell Biol* 2007; **8**: 613–621.
- 14 Edgar BA. From cell structure to transcription: Hippo forges a new path. *Cell* 2006; **124**: 267–273.
- 15 Zhao B, Li L, Lei Q, Guan KL. The Hippo-YAP pathway in organ size control and tumorigenesis: an updated version. *Genes Dev* 2010; **24**: 862–874.
- 16 Dong J, Feldmann G, Huang J, Wu S, Zhang N, Comerford SA et al. Elucidation of a universal size-control mechanism in *Drosophila* and mammals. *Cell* 2007; **130**: 1120–1133.
- 17 Oh H, Irvine KD. *In vivo* regulation of Yorkie phosphorylation and localization. *Development* 2008; **135**: 1081–1088.
- 18 Zhao B, Wei X, Li W, Udan RS, Yang Q, Kim J et al. Inactivation of YAP oncoprotein by the Hippo pathway is involved in cell contact inhibition and tissue growth control. *Genes Dev* 2007; **21**: 2747–2761.
- 19 Steinhart AA, Gayyed MF, Klein AP, Dong J, Maitra A, Pan D et al. Expression of Yes-associated protein in common solid tumors. *Hum Pathol* 2008; **39**: 1582–1589.
- 20 Wang K, Degerny C, Xu M, Yang XJ. YAP, TAZ, and Yorkie: a conserved family of signal-responsive transcriptional coregulators in animal development and human disease. *Biochem Cell Biol* 2009; **87**: 77–91.
- 21 Zheng T, Wang J, Jiang H, Liu L. Hippo signaling in oval cells and hepatocarcinogenesis. *Cancer Lett* 2011; **302**: 91–99.
- 22 Xu MZ, Yao TJ, Lee NP, Ng IO, Chan YT, Zender L et al. Yes-associated protein is an independent prognostic marker in hepatocellular carcinoma. *Cancer* 2009; **115**: 4576–4585.
- 23 O'Neill E, Rushworth L, Baccarini M, Kolch W. Role of the kinase MST2 in suppression of apoptosis by the proto-oncogene product Raf-1. *Science* 2004; **306**: 2267–2270.
- 24 O'Neill E, Kolch W. Taming the Hippo: Raf-1 controls apoptosis by suppressing MST2/Hippo. *Cell Cycle* 2005; **4**: 365–367.
- 25 Romano D, Matallanas D, Weitsman G, Preisinger C, Ng T, Kolch W. Proapoptotic kinase MST2 coordinates signaling crosstalk between RASSF1A, Raf-1, and Akt. *Cancer Res* 2010; **70**: 1195–1203.
- 26 Doggett K, Grusche FA, Richardson HE, Brumby AM. Loss of the *Drosophila* cell polarity regulator Scribbled promotes epithelial tissue overgrowth and cooperation with oncogenic Ras-Raf through impaired Hippo pathway signaling. *BMC Dev Biol* 2011; **11**: 57.
- 27 Lee SJ, Lee MH, Kim DW, Lee S, Huang S, Ryu MJ et al. Cross-regulation between oncogenic BRAF(V600E) kinase and the MST1 pathway in papillary thyroid carcinoma. *PLoS One* 2011; **6**: e16180.
- 28 Kim NG, Koh E, Chen X, Gumbiner BM. E-cadherin mediates contact inhibition of proliferation through Hippo signaling-pathway components. *Proc Natl Acad Sci USA* 2011; **108**: 11930–11935.
- 29 Zhao B, Ye X, Yu J, Li L, Li W, Li S et al. TEAD mediates YAP-dependent gene induction and growth control. *Genes Dev* 2008; **22**: 1962–1971.
- 30 Ito T, Seyama T, Hayashi Y, Hayashi T, Dohi K, Mizuno T et al. Establishment of 2 human thyroid-carcinoma cell-lines (8305c, 8505c) bearing p53 gene-mutations. *Int J Oncol* 1994; **4**: 583–586.
- 31 Ceraline J, Deplanque G, Noel F, Natarajan-Ame S, Bergerat JP, Klein-Soyer C. Sensitivity to cisplatin treatment of human K1 thyroid carcinoma cell lines with altered p53 function. *Cancer Chemother Pharmacol* 2003; **51**: 91–95.
- 32 Wan PT, Garnett MJ, Roe SM, Lee S, Niculescu-Duvaz D, Good VM et al. Mechanism of activation of the RAF-ERK signaling pathway by oncogenic mutations of B-RAF. *Cell* 2004; **116**: 855–867.
- 33 Gild ML, Bullock M, Robinson BG, Clifton-Bligh R. Multikinase inhibitors: a new option for the treatment of thyroid cancer. *Nat Rev Endocrinol* 2011; **7**: 617–624.
- 34 Downward J. Targeting RAF: trials and tribulations. *Nat Med* 2011; **17**: 286–288.
- 35 Nucera C, Nehs MA, Mekel M, Zhang X, Hodin R, Lawler J et al. A novel orthotopic mouse model of human anaplastic thyroid carcinoma. *Thyroid* 2009; **19**: 1077–1084.
- 36 Raveh S, Gavert N, Ben-Ze'ev A. L1 cell adhesion molecule (L1CAM) in invasive tumors. *Cancer Lett* 2009; **282**: 137–145.
- 37 Gavert N, Conacci-Sorrell M, Gast D, Schneider A, Altevogt P, Brabletz T et al. L1, a novel target of beta-catenin signaling, transforms cells and is expressed at the invasive front of colon cancers. *J Cell Biol* 2005; **168**: 633–642.
- 38 Konsavage Jr WM, Kyler SL, Rennoll SA, Jin G, Yochum GS. Wnt/beta-catenin signaling regulates Yes-associated protein (YAP) gene expression in colorectal carcinoma cells. *J Biol Chem* 2012; **287**: 11730–11739.
- 39 Kim KS, Min JK, Liang ZL, Lee K, Lee JU, Bae KH et al. Aberrant I1 cell adhesion molecule affects tumor behavior and chemosensitivity in anaplastic thyroid carcinoma. *Clin Cancer Res* 2012; **18**: 3071–3078.
- 40 Lee JH, Kim TS, Yang TH, Koo BK, Oh SP, Lee KP et al. A crucial role of WW45 in developing epithelial tissues in the mouse. *EMBO J* 2008; **27**: 1231–1242.
- 41 Liu AM, Xu MZ, Chen J, Poon RT, Luk JM. Targeting YAP and Hippo signaling pathway in liver cancer. *Expert Opin Ther Targets* 2010; **14**: 855–868.
- 42 Heallen T, Zhang M, Wang J, Bonilla-Claudio M, Klysiak E, Johnson RL et al. Hippo pathway inhibits Wnt signaling to restrain cardiomyocyte proliferation and heart size. *Science* 2011; **332**: 458–461.
- 43 Zhao B, Tumaneng K, Guan KL. The Hippo pathway in organ size control, tissue regeneration and stem cell self-renewal. *Nat Cell Biol* 2011; **13**: 877–883.
- 44 Genevet A, Tapon N. The Hippo pathway and apico-basal cell polarity. *Biochem J* 2011; **436**: 213–224.
- 45 Genevet A, Wehr MC, Brain R, Thompson BJ, Tapon N. Kibra is a regulator of the Salvador/Warts/Hippo signaling network. *Dev Cell* 2010; **18**: 300–308.
- 46 Willecke M, Hamaratoglu F, Kango-Singh M, Udan R, Chen CL, Tao C et al. The fat cadherin acts through the hippo tumor-suppressor pathway to regulate tissue size. *Curr Biol* 2006; **16**: 2090–2100.
- 47 Yokoyama T, Osada H, Murakami H, Tatematsu Y, Taniguchi T, Kondo Y et al. YAP1 is involved in mesothelioma development and negatively regulated by Merlin through phosphorylation. *Carcinogenesis* 2008; **29**: 2139–2146.
- 48 Oh HJ, Lee KK, Song SJ, Jin MS, Song MS, Lee JH et al. Role of the tumor suppressor RASSF1A in Mst1-mediated apoptosis. *Cancer Res* 2006; **66**: 2562–2569.
- 49 Zhang H, Liu CY, Zha ZY, Zhao B, Yao J, Zhao S et al. TEAD transcription factors mediate the function of TAZ in cell growth and epithelial-mesenchymal transition. *J Biol Chem* 2009; **284**: 13355–13362.
- 50 Chan SW, Lim CJ, Huang C, Chong YF, Gunaratne HJ, Hogue KA et al. WW domain-mediated interaction with Wbp2 is important for the oncogenic property of TAZ. *Oncogene* 2011; **30**: 600–610.
- 51 Zhao B, Li L, Lu Q, Wang LH, Liu CY, Lei Q et al. Angiomotin is a novel Hippo pathway component that inhibits YAP oncoprotein. *Genes Dev* 2011; **25**: 51–63.
- 52 Chan SW, Lim CJ, Chong YF, Pobbati AV, Huang C, Hong W. Hippo pathway-independent restriction of TAZ and YAP by angiomotin. *J Biol Chem* 2011; **286**: 7018–7026.
- 53 Wrighton KH. Mechanotransduction: YAP and TAZ feel the force. *Nat Rev Mol Cell Biol* 2011; **12**: 404.
- 54 Pritchard CA, Hayes L, Wojnowski L, Zimmer A, Marais RM, Norman JC. B-Raf acts via the ROCKII/LIMK/cofilin pathway to maintain actin stress fibers in fibroblasts. *Mol Cell Biol* 2004; **24**: 5937–5952.
- 55 Kirui JK, Xie Y, Wolff DW, Jiang H, Abel PW, Tu Y. Gbetagamma signaling promotes breast cancer cell migration and invasion. *J Pharmacol Exp Ther* 2010; **333**: 393–403.
- 56 Lehtinen L, Vainio P, Wikman H, Reemts J, Hilvo M, Issa R et al. 15-Hydroxyprostaglandin dehydrogenase associates with poor prognosis in breast cancer, induces epithelial-mesenchymal transition, and promotes cell migration in cultured breast cancer cells. *J Pathol* 2012; **226**: 674–686.
- 57 Lee KP, Lee JH, Kim TS, Kim TH, Park HD, Byun JS et al. The Hippo-Salvador pathway restrains hepatic oval cell proliferation, liver size, and liver tumorigenesis. *Proc Natl Acad Sci USA* 2010; **107**: 8248–8253.
- 58 Nikiforov YE. Genetic alterations involved in the transition from well-differentiated to poorly differentiated and anaplastic thyroid carcinomas. *Endocr Pathol* 2004, Winter **15**: 319–327.
- 59 Jo YS, Huang S, Kim YJ, Lee IS, Kim SS, Kim JR et al. Diagnostic value of pyrosequencing for the BRAF V600E mutation in ultrasound-guided fine-needle aspiration biopsy samples of thyroid incidentalomas. *Clin Endocrinol (Oxf)* 2009; **70**: 139–144.
- 60 Stoeltzing O, Liu W, Reinmuth N, Fan F, Parikh AA, Bucana CD et al. Regulation of hypoxia-inducible factor-1alpha, vascular endothelial growth factor, and angiogenesis by an insulin-like growth factor-I receptor autocrine loop in human pancreatic cancer. *Am J Pathol* 2003; **163**: 1001–1011.



Oncogenesis is an open-access journal published by Nature Publishing Group. This work is licensed under a Creative Commons Attribution-NonCommercial-NoDerivs 3.0 Unported License. To view a copy of this license, visit <http://creativecommons.org/licenses/by-nc-nd/3.0/>

Supplementary Information accompanies this paper on the Oncogenesis website (<http://www.nature.com/oncsis>)